Nanotechnology Perceptions
ISSN 1660-6795
www.nano-*ntp.com*

Wear Behaviour Optimization Of A356-Sn/Al_2O_3 Composites Using Box–Behnken Design

Veera Ajay C[1*], Boopathi C[2], Vinoth V[3], Karthikeyan L[1], Santhosh Velmurugan[4]

[1]*National Engineering College, Kovilpatti, India.*
[2]*Bannari Amman Institute of Technology, Sathyamangalam, Tamilnadu, India.*
[3]*Easwari Engineering College, Chennai, Tamilnadu, India*
[4]*Karpagam Academy of Higher Education Coimbatore, Tamil Nadu, India.*
**ajayveera2@gmail.com*

The increasing demand for advanced engineering materials across various manufacturing sectors has led to significant interest in metal matrix composites due to their excellent characteristics. This study examines the wear characteristics of A356 alloy-based composites reinforced with aluminum dioxide (Al_2O_3) and tin (Sn) particulates. A356-Sn/Al_2O_3 composites were fabricated using the stir casting method, incorporating 10 wt.% Al_2O_3 and varying Sn content (0, 4, and 8 wt.%). The addition of Sn, along with Al_2O_3, enhanced the wear characteristics of the developed composites. Optimal values were determined using Box–Behnken based Response Surface Methodology (RSM) by analyzing Wear Rate (WR) and Coefficient of Friction (COF). The study considered Sn wt.% (0, 4, 8), normal load (10, 20, 30 N), and Sliding Speed (SS) (1, 2, 3 m/s) to establish the best combination for improved wear resistance. ANOVA was used to determine the most influential parameters affecting the COF and wear rate. The results demonstrated that Sn content played a crucial role in enhancing the wear resistance of the composites.

Keyworks: hypo eutectic A356 alloy; Al_2O_3; Sn; Box–Behnken design, Wear loss; COF.

1. Introduction

Aluminum Metal Matrix Composites (AMMCs) have gained significant attention due to their enhanced mechanical and physical properties, including low density, high stiffness, superior strength-to-weight ratio, excellent machinability, and high formability [1]. These attributes, combined with simple fabrication techniques, make AMMCs highly suitable for various industrial applications. To improve the properties of aluminum alloys, ceramic reinforcements in micro or nano forms are commonly incorporated. Reinforcement materials such as silicon carbide (SiC) [2, 3], boron carbide (B_4C) [4, 5], graphite (Gr) [6, 7], aluminum oxide (Al_2O_3) [8, 9], tin (Sn) [10, 11, 12], silicon nitride [13], titanium dioxide (TiO_2) [14] and tungsten carbide (WC) [15] are widely used due to their ability to enhance strength, hardness, and wear resistance. Among these, Al_2O_3 is particularly notable for its superior mechanical properties, making it suitable for applications in pistons, cylinder heads, brake pads, gears, bearings, and bushings. The A356

aluminum alloy is frequently utilized in industrial applications due to its excellent strength, hardness, and toughness compared to other aluminum alloys. The addition of ceramic reinforcements further enhances its properties, making it an ideal material for demanding applications in sectors such as aerospace, automotive, marine, and defense. Additionally, lubrication is a critical requirement in many engineering applications to reduce friction and wear. Tin (Sn) particles are often incorporated into AMMCs to provide self-lubricating properties and enhance wear resistance. The synergistic effect of ceramic and metallic reinforcements in AMMCs leads to improved mechanical performance, making them highly desirable for advanced engineering applications.

2. Experimental Procedure

The A356 alloy was used as the matrix, with alumina (Al_2O_3) and tin (Sn) powders as reinforcements, both having high purity (>99%) and average sizes of 40 µm and 50 µm, respectively. Using stir-casting, 500 g of A356 was melted at 700°C, stirred at 500 rpm, and mixed with preheated Sn and Al_2O_3 powders. Sn was preheated under argon to prevent oxidation and dissolved at 850°C over 6 hours, while Al_2O_3 was added to ensure even dispersion. The composite mix was cast into a steel die. This research focuses on 10 wt% Al_2O_3, varying Sn at 0, 3, and 6 wt% to improve material properties. Table 1 shows the composition of composites. The selection of 10% Al_2O_3 in the composition of composites was based on earlier literature [16, 17] and a pilot study. These studies demonstrated that reinforcing aluminum with 10% micron-sized Al_2O_3 significantly enhanced the properties. Therefore, in the present research, the Al_2O_3 content was fixed at 10%, while the Sn content was varied from 0 to 8 wt.%.

Table 1. Composition of Composites

Al_2O_3	Tin	A356 alloy
10 wt.%	0 wt.%	90 wt.%
10 wt.%	4 wt.%	86 wt.%
10 wt.%	8 wt.%	82 wt.%

Dry sliding wear tests were performed using a Ducom TR-20LE pin-on-disc setup, following the ASTM G99 standard by considering a constant sliding distance of 2000 m under varying loads and sliding velocity. Wear loss and friction coefficients were determined by weighing the pin before and after each test using a precision balance with 0.001 g accuracy. Table 2 displays the parameters considered for the current study.

Table 2. Input factors and corresponding responses

Ex.No	Weight percentage of Sn	Load	SS	WR	COF
	%	N	m/s	g/km	
1	8	20	1	0.018	0.28
2	4	20	2	0.044	0.39

3	8	20	3	0.024	0.32
4	0	30	2	0.08	0.58
5	4	10	1	0.037	0.36
6	0	20	1	0.068	0.49
7	3	20	2	0.046	0.39
8	8	30	2	0.035	0.35
9	0	20	3	0.072	0.52
10	4	30	3	0.054	0.45
11	4	30	1	0.051	0.42
12	4	20	2	0.046	0.42
13	4	20	2	0.048	0.41
14	8	10	2	0.014	0.3
15	4	20	2	0.044	0.42
16	4	10	3	0.04	0.38
17	0	10	2	0.062	0.46

3. Results and Discussion

3.1. Statistical Evaluation on WR of A356-Sn/Al_2O_3 Composites

In Table 3, among the individual factors, A-Wt % of Sn is the most influential on wear rate, showing the highest significance with a Fisher's ratio of 703.21 and a probability value of < 0.0001. B-Load (N) is also highly significant, with a Fisher's ratio of 87.18 and a probability value of < 0.0001. Meanwhile, C-Sliding speed (m/s), though less influential, has a statistically significant effect on wear rate, with a Fisher's ratio of 4.97 and a probability value of 0.0440. The residual value is low, indicating minimal unexplained variance.

Table 3: ANOVA for WR

Terms	Sum of Squares (SS)	df	Mean Square (MS)	F Value	p-value
Model	0.005119	3	0.001706	265.1187	< 0.0001
Weight Percentage of Sn	0.004526	1	0.004526	703.2051	< 0.0001
Load	0.000561	1	0.000561	87.17931	< 0.0001
SS	0.000032	1	0.000032	4.971687	0.0440
Residual	8.37E-05	13	6.44E-06		
Lack of Fit	7.27E-05	10	7.27E-06	1.982013	0.3123
Pure Error	0.000011	3	3.67E-06		
Cor Total	0.005203	16			

The regression models for WR are highly accurate, with R-squared values of 0.9839, indicating a strong fit and reliable predictive capability. The predictive mathematical models for wear rate are mentioned in equation 1.

Wear rate (g/Km) = +0.048659 - 5.92473E-003 * Wt % of Sn + 8.37500E-004 * Load (N) + 2.00000E-003 * Sliding speed (m/s)
(1)

The normal probability plot (Figure 1) confirms that both residuals and the predicted model responses are normally distributed. The residuals align closely with a straight line, suggesting that random errors follow a normal distribution.

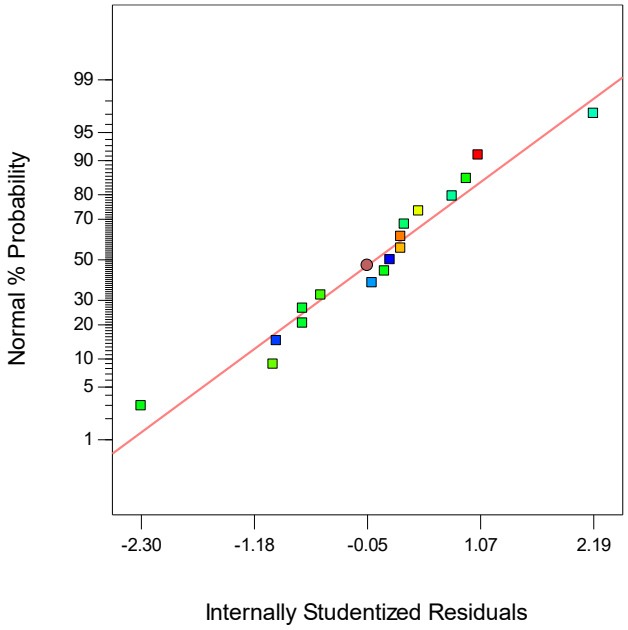

Figure 1. Residual Plot for WR

3.2. Surface Plot of wear rates against input factors

The impact of process parameters on the WR of A356/Al_2O_3/Sn composites was evaluated through dry sliding wear tests, as shown in Figures 2a, 2b, and 2c. Results indicate that increasing both the load and the Sn weight percentage raises the wear rate, particularly at 30 N, as shown in Figure 2a. This increase is likely due to adhesive wear, caused by higher temperatures between contact surfaces under greater loads. At 30 N, a protective oxide layer, called a mechanically mixed layer, may form as Al_2O_3 and Sn particles are removed from the composite, reducing wear at higher sliding velocities. As the velocity increases, the wear rate initially rises due to this protective layer formation.

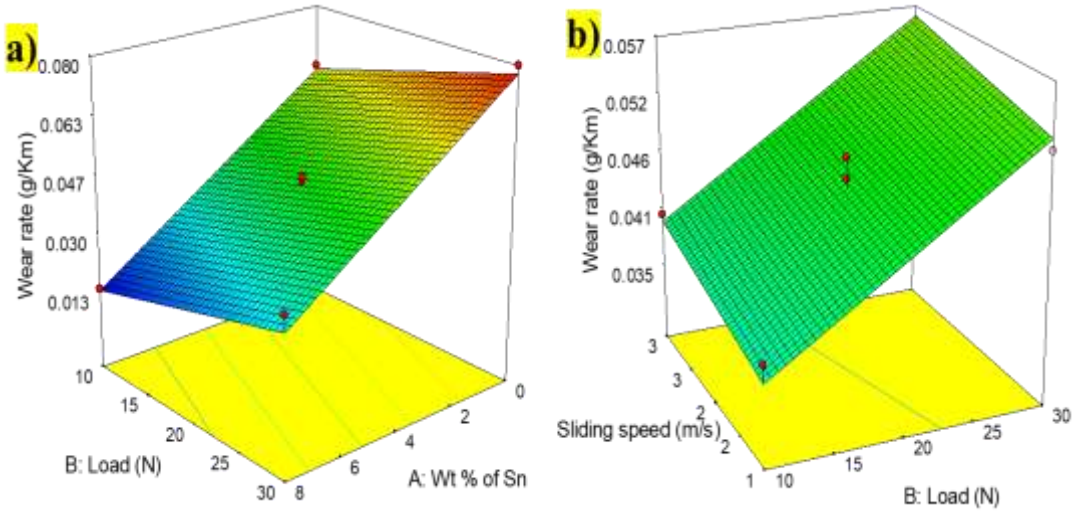

Figure 2. 3D surface plot of Wear rate

3.3. Statistical Evaluation on COF of A356-Sn/Al_2O_3 Composites

In Table 4, among the individual factors, A-Wt % of Sn has the largest influence on wear rate, with a Fisher's ratio of 200.7809 and a probability value of < 0.0001, establishing it as the most significant factor; B-Load (N) is also highly significant, with a Fisher's ratio of 28.76937 and a probability value of < 0.0001; and C-Sliding speed (m/s) has a lower a Fisher's ratio of 4.6031 and a probability value of 0.0514, indicating a weaker and marginally significant effect on wear rate. The residual value is low, indicating minimal unexplained variance.

Table 4: ANOVA for COF

Terms	SS	df	MS	F Value	p-value
Model	0.091564	3	0.030521	78.05112	< 0.0001
Weight Percentage of Sn	0.078514	1	0.078514	200.7809	< 0.0001
Load	0.01125	1	0.01125	28.76937	0.0001
SS	0.0018	1	0.0018	4.6031	0.0514
Residual	0.005084	13	0.000391		
Lack of Fit	0.004484	10	0.000448	2.241766	0.2746
Pure Error	0.0006	3	0.0002		
Cor Total	0.096647	16			

The regression models for CoF were highly accurate, with R-squared values of 0.9474, indicating a strong fit and reliable predictive capability. The predictive mathematical models for COF are mentioned in equation 2.

COF = 0.40049 - 0.024676 * Wt % of Sn + 3.75000E-003 * Load (N) + 0.015000 * Sliding speed (m/s)

(2)

The normal probability plot (Figure 3) confirms that both residuals and the predicted model responses are normally distributed. The residuals align closely with a straight line, suggesting that random errors follow a normal distribution.

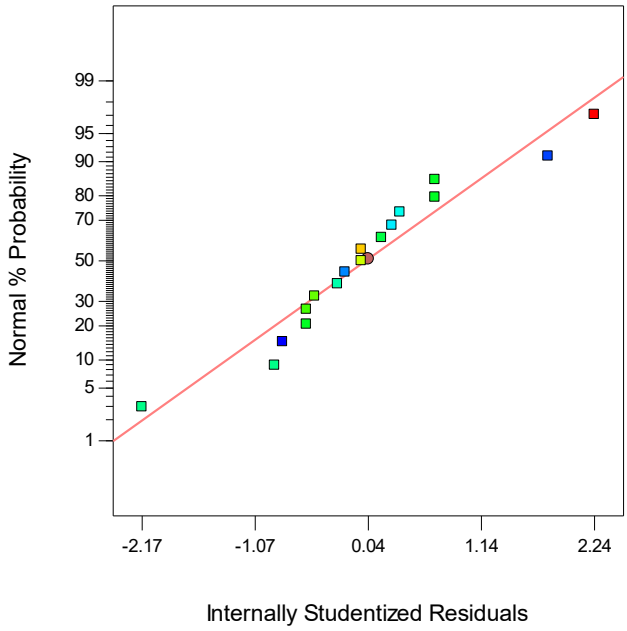

Figure 3. Residual Plot for COF

3.4. Surface Plot of COF against input factors

The impact of wear parameters on the CoF for A356/Al_2O_3/Sn composites was examined using dry sliding wear tests, with results shown in Figure 4. As depicted in Figure 4b, the CoF increases with higher loads and sliding speeds. At a velocity of 1 m/s and an applied load of 10 N, the CoF is lower, attributed to the formation of a third body layer from abrasive material removal at lower velocities. However, as the load increases from 10 N to 30 N, the CoF rises. This occurs because the tin-based transfer layer, which acts as a solid lubricant, remains stable at lower loads but deteriorates under higher loads due to increased temperatures.

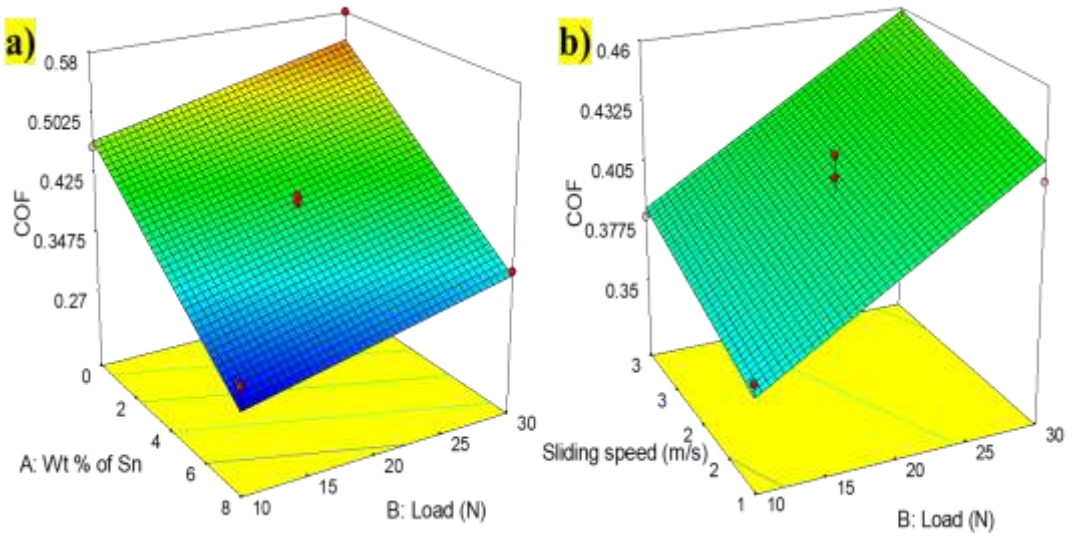

Figure 4. 3D surface plot of COF

3.5. Performance Characteristic Optimization Using the Desirability Function

The desirability approach aims to find the optimal processing conditions that meet all the goals for tin wt%, load, and sliding speed while minimizing wear rates and COF. A desirability value of 1.0 is not essential, as it depends on how closely the upper bound and lower bound align with the actual optimal values. Figures 5 and 7 show a ramp and bar graph of desirability, respectively, illustrating how closely the results approach the target. Dots on the ramp graph represent process parameter settings or predicted performance, while the height of the bars shows each response's desirability. The linear ramp function between low and high values indicates that the weight for each factor was set to one. The desirability, ranging from 0 to 1, reflects how well the system meets the design criteria, with values closer to 1 indicating better performance.

3D desirability surface plots were created to evaluate processing variables within the specified range, aiming for minimal performance characteristics. Figure 6 shows how sliding speed and reinforcement percentage affect the desirability function. The overall desirability was lower at high reinforcement content and low sliding speeds, with an optimal region identified at the peak, where the desirability reached a maximum of 1. This value decreased nonlinearly moving away from the peak, indicating how closely the results align with the desired objectives.

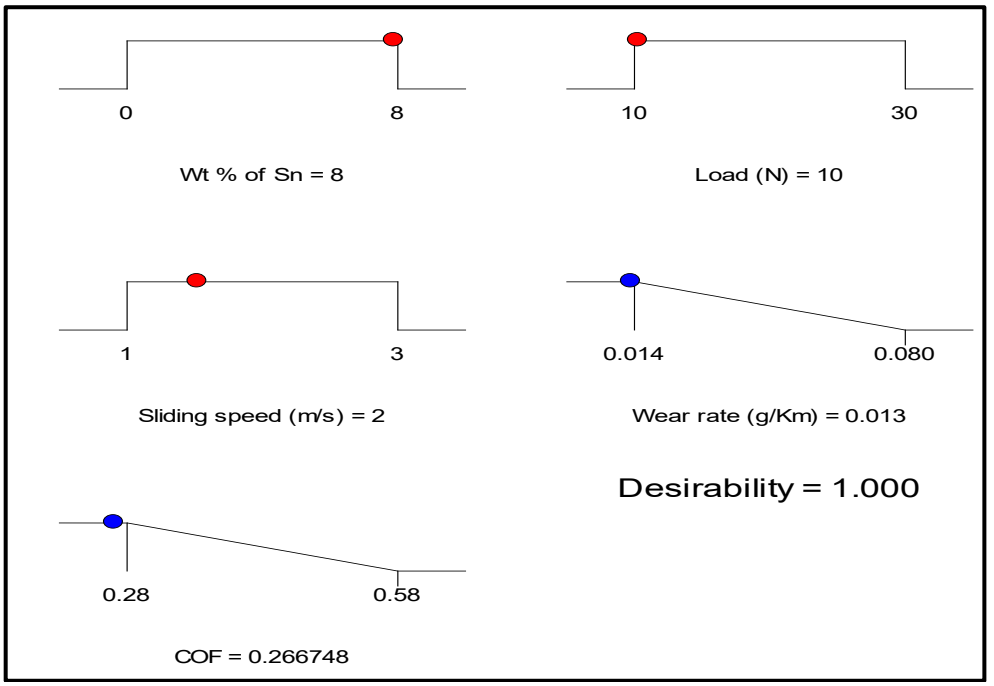

Fig. 5 Ramp function plot of Desirability for the A356-Sn/Al_2O_3

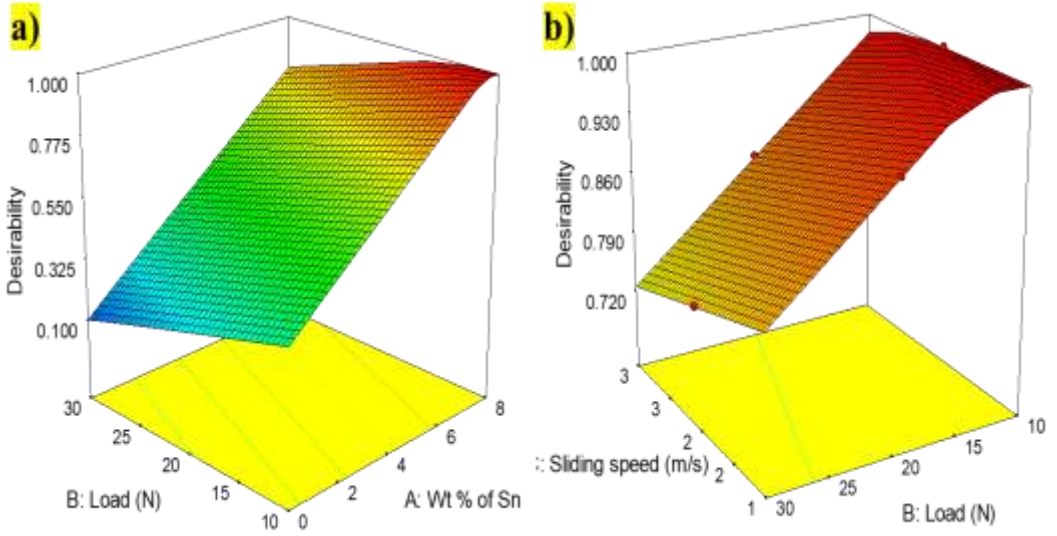

Fig. 6 3D Surface plot of the desirability of A356-Sn/Al_2O_3

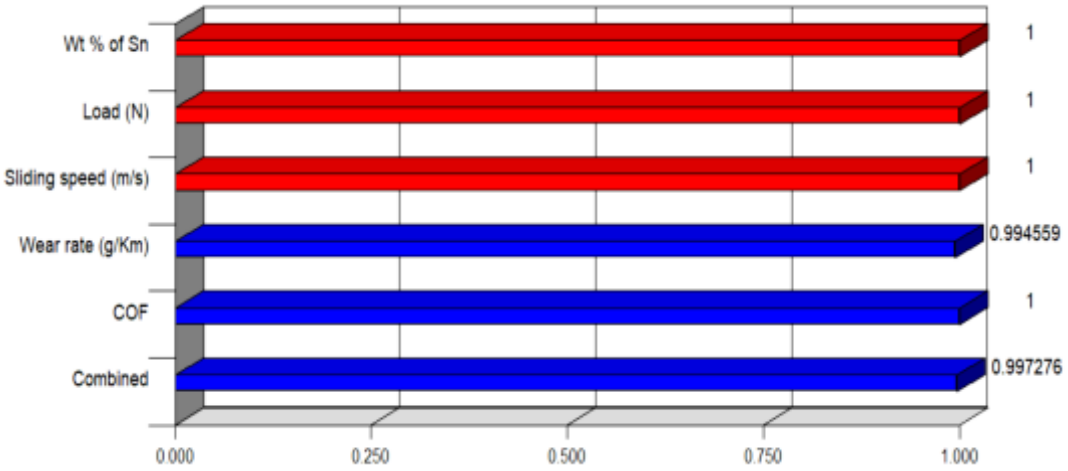

Fig. 7 Bar graph of Desirability for the A356-Sn/Al_2O_3

4. Conclusion

The study evaluated the effects of applied load, sliding speed, and Sn content on the WR and CoF of A356/Al_2O_3/Sn composites using dry sliding wear tests.

1) ANOVA results demonstrated that Sn content has the most significant impact on WR and CoF, followed by applied load and sliding speed, with high statistical significance and minimal unexplained variance.
2) The regression models for WR and CoF were highly accurate, with R-squared values of 0.9839 and 0.9474, respectively, indicating a strong fit and reliable predictive capability.
3) Surface plot study exposed that WR increased with higher load and Sn content.
4) The CoF increased with rising load and speed, with lower values observed at 1 m/s and 10 N due to the formation of a tin-based transfer layer that deteriorates under higher loads.
5) Residual plots confirmed that the models' errors were normally distributed, supporting the models' validity and the absence of irregular patterns or significant deviations.
6) Optimization using the desirability function identified an optimal combination of 8 wt% Sn, 11 N load, and 1 m/s sliding speed, achieving minimal wear rate and CoF with a maximum desirability score of 1.

Reference

1. C.S. Ramesh, S. Pramod, R. Keshavamurthy, A study on microstructure and mechanical properties of Al 6061–TiB_2 in-situ composites, Mater. Sci. Eng. A. 528 (2011) 4125–4132.
2. M.R. Morovvati, A. Lalehpour, A. Esmaeilzare, Effect of nano/micro-B_4C and SiC particles on fracture properties of aluminum 7075 particulate composites under chevron-notch plane strain fracture toughness test, Mater. Res. Express. 3 (2016) 1250.
3. C. Kannan, R. Ramanujam, K. Venkatesan, et al., An investigation on the tribological characteristics of Al 7075-based single and hybrid nanocomposites, Mater. Today: Proc. 5 (2018) 12837−12847.
4. V.M. Ravindranath, G.S. Shankar, S. Basavarajappa, et al., Dry sliding wear behavior of hybrid aluminum metal matrix composite reinforced with boron carbide and graphite particles, Mater. Today: Proc. 4 (10) (2017) 11163–11167.

5. A.E.P.A. Baradeswaran, A.E. Perumal, Influence of B_4C on the tribological and mechanical properties of Al 7075–B_4C composites, Compos. B, Eng. 54 (2013) 146–152.
6. C.V. Ajay, A.A.M. Moshi, Investigation and optimization of the tribological parameters of hypoeutectic A356/Gr/Sn metal matrix composites using grey-fuzzy and ANN modeling methods, J. Fail. Anal. Preven. 24 (2024) 1916–1933. https://doi.org/10.1007/s11668-024-01978-8.
7. C.V. Ajay, K. Thoufiq Mohammed, P. Hariharasakthisudhan, V. Nantha Kumar, R. Vishnu, Characteristics study of mechanical and tribological behaviour of Gr/Sn dispersed Al-7Si alloy matrix composite processed through bottom pouring stir casting technique, Silicon 15 (2023) 5089–5104. https://doi.org/10.1007/s12633-023-02422-6.
8. C.V. Ajay, P. Hariharasakthisudhan, S. Anand, I. Sivasubramanian, Mechanical and tribological characteristics of hypoeutectic Al-7Si alloy-based composite reinforced with Sn metal powder and Al_2O_3 using bottom pouring stir casting technique, Phys. Scr. 98 (11) (2023).
9. C.V. Ajay, P. Hariharasakthisudhan, V. Vinoth, S. Sundaravignesh, Influence of process parameters on the tribological behaviour of dual reinforcement (Al_2O_3/Si_3N_4) in AA6061 metal matrix composite, Mater. Today: Proc. (2023). https://doi.org/10.1016/j.matpr.2023.08.230.
10. C.V. Ajay, K. Manisekar, A. Andrews, Investigating and predicting tribological characteristics of AZ31 alloy composites reinforced with nano-Al_2O_3 and micro-Sn particles: a comparative analysis using CCD-RSM and ANN models, Phys. Scr. 99 (8) (2024).
11. C.V. Ajay, K. Manisekar, K.T. Mohammed, In vitro degradation and dry sliding wear behaviour of AZ31-Sn/Al_2O_3 nano metal matrix composites in simulated body fluid for biomedical application, Proc. Inst. Mech. Eng. Part L: J. Mater. Des. Appl. 238 (1) (2024) 148-159. https://doi.org/10.1177/14644207231188226.
12. C.V. Ajay, K. Manisekar, Metallurgical, mechanical, and tribological properties of AZ31-Sn/nano-Al_2O_3 composites fabricated by stir casting technique, Trans. Indian Inst. Met. 76 (2023) 1819–1830. https://doi.org/10.1007/s12666-023-02879-4.
13. C.V. Ajay, K. Manisekar, K.T. Mohammed, Influence of silicon nitride (Si_3N_4) reinforcement on mechanical properties and wear behaviour of AZ31–nano alumina (Al_2O_3) composites developed through the stir casting route, Phys. Scr. 99 (4) (2024). https://doi.org/10.1088/1402-4896/ad3025.
14. J. Yadu Krishnan, K. Thoufiq Mohammed, C.V. Ajay, K. Manisekar, Study on the wear behaviour of magnesium metal matrix composites reinforced with titanium dioxide (TiO_2), in: Lecture Notes in Mechanical Engineering, Springer, Singapore, 2023. https://doi.org/10.1007/978-981-19-3895-5_53.
15. D. Vignesh Kumar, S. Arulselvan, A. Arul Marcel Moshi, C.V. Ajay, P. Balamurugan, Mechanical characterization and frictional wear behavior analysis on nano tungsten carbide and molybdenum disulfide particles reinforced aluminum 7075 composites, Proc. Inst. Mech. Eng. Part E: J. Process Mech. Eng. 238 (3) (2024) 1185-1194. https://doi.org/10.1177/09544089221150726.
16. S.A. Sajjadi, H.R. Ezatpour, M.T. Parizi, Comparison of microstructure and mechanical properties of A356 aluminum alloy/Al_2O_3 composites fabricated by stir and compocasting processes, Mater. Des. 34 (2012) 106–111.
17. A.H. Hallem, T.A. Jasim, N.S. Radhi, Effect of alumina reinforcement on some mechanical properties of aluminum matrix composites produced by stir casting process, Int. J. Civ. Eng. Technol. (IJCIET). 9 (10) (2018) 1271–1280.